Kinetic roughening of a terrace ledge

Tim Salditt and Herbert Spohn
Theoretische Physik, Ludwig-Maximilians-Universität, Theresienstrasse 37, 8 München 2, Germany
(Received 29 December 1992)

We study the motion of an isolated terrace ledge on a crystalline surface within the framework of the terrace-ledge-kink model. We argue that for length scales larger than the diffusion length the step roughness is governed by the Kardar-Parisi-Zhang (KPZ) equation that predicts a broadening as $t^{1/3}$. For smaller length scales a variety of possibilities are explored. Their occurrence depends sensitively on the rates for the adsorption and desorption processes both on the terraces and at the ledge. The ledge could be unstable, developing a fractal, dendritic type of structure. If the ledge is stable, we obtain a crossover from a $t^{1/6}$ (conserved dynamics, model B) to a $t^{1/4}$ (nonconserved dynamics, model A) and a $t^{1/3}$ (KPZ) broadening.

PACS number(s): 82.20.Wt, 61.50.Cj, 05.40.+j, 68.55.Bd

I. INTRODUCTION

In a classical paper, Burton, Cabrera, and Frank (BCF) [1] studied the motion of a terrace ledge on a vicinal crystal surface. They considered an isolated step taking into account, on the level of a continuum theory, the following processes: (i) From the ambient atmosphere, atoms absorb onto and desorb off the crystalline surface. (ii) Atoms diffuse on the crystalline surface. (iii) Atoms can attach to, respectively detach from, the ledge, diffuse along the ledge, and stick at kink sites. BCF assumed the ledge to be straight and to act as a perfect sink for the atoms on the terraces. They then computed the ledge velocity. The BCF theory has been extended to the cases where the step is no longer a perfect sink and where steps are not infinitely far apart [2].

The BCF theory does not address the atomic structure of the ledge at all. In fact, experiments show that, under certain conditions when growing, the ledge may develop instabilities and is certainly not straight, even on the average [3]. The purpose of our paper is to explore some of the possible microstructures. Our main focus is the roughness of the moving ledge. In particular, we will also exhibit examples where the ledge becomes fractal on a length scale small compared to the diffusion length.

By necessity, a microscopic model must be based on drastic simplifications. We assume here a simple cubic lattice with a high-symmetry surface, and imagine that somehow a perfectly straight ledge oriented along one of the axes has been prepared initially. The crystal step has the height of a single atomic layer and separates a lower from an upper terrace. In our Monte Carlo simulations, the ledge moves upwards. Thus the upper terrace corresponds to the back and the lower to the front terrace, cf. Fig. 1. We stay within the BCF frame in assuming the following atomistic processes: (i) On the terraces atoms are created and disappear with certain rates. (ii) Atoms jump to neighboring lattice sites. (iii) Atoms detach from and attach to the ledge with given rates. Atoms jump along the ledge, move around corners, and stick at kink sites. Bulk overhangs are forbidden. We thereby have defined the terrace-ledge-kink (TLK) model, cf. Sec. II for more details. The problem posed then is to understand how in the TLK model a crystal step advances in the course of time.

Even if we require detailed balance for the transition rates, we still have a fairly large space of parameters, and it is not feasible to explore "all" possibilities. First of all, there could be nucleation on the terraces. Of course, the ledge will then disappear. Therefore we have to restrict ourselves to a fairly low density of adatoms on the terraces. The aggregation of atoms at the ledge is diffusion limited. Thus we expect fractal, dentriticlike structures on a scale smaller than the diffusion length. We will

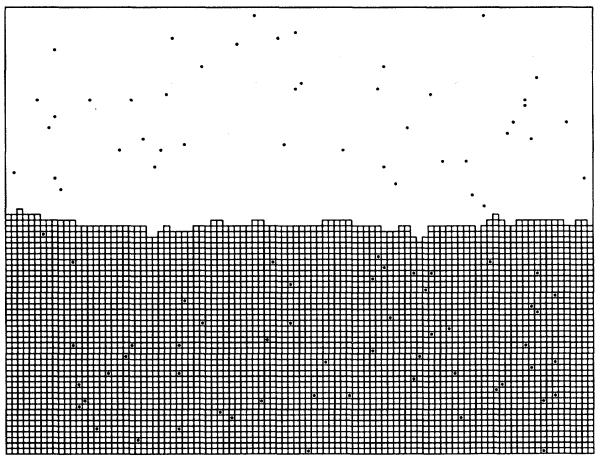

FIG. 1. Typical configuration with the high-density phase (lower half) growing towards the low-density phase (upper half) at $t=10^4$ MCS. A 100×80 section of a 128×128 lattice is shown. About eight monatomic layers have grown. The imposed flux is $F=3\times10^{-5}$ (site$\times$MCS)$^{-1}$, the diffusion length $x_D=26a$, and the temperature $\beta J=7$. A square represents an occupation number 1 of a site with occupied neighbors, a dot represents an isolated occupation number 1 (mobile adatom on the front terrace), and a square with a dot inside corresponds to an occupation number 2 (mobile adatom on the back terrace).

present some examples in Sec. VI. On the other hand, ledge diffusion has the effect to stabilize the front. There is a regime in parameter space where the ledge remains straight on the average (Sec. III). The ledge roughness can then be studied within the framework of linear fluctuation theory. This is carried through in Sec. IV. As known from the work of Kardar, Parisi, and Zhang (KPZ) [4], even for stable growth the systematic part of the local velocity introduces nonlinearities into the equations of motion, which lead to a $t^{1/3}$ power law for the broadening. For a moving ledge this mechanism is in operation and we estimate the time when it will dominate (Sec. V).

II. THE TERRACE-LEDGE-KINK MODEL AS A DRIVEN INTERFACE

We assume a simple cubic lattice. At sufficiently low temperatures, bulk overhangs can be ignored. Thus we can introduce the reference plane $(aZ)^2$ with lattice constant a. At each site $i \in Z^2$, $i=(i_1,i_2)$, there is a height variable $\zeta_i=0,1,2$. A height configuration $\{\zeta_i\}$ is abbreviated by ζ. As an example, a straight ledge along the x axis is given by $\zeta_i=0$ for $i_2>0$, $\zeta_i=1$ for $i_2\leq 0$. An adatom on the back terrace would correspond to $\zeta_i=2$. To each bond we associate a binding energy J. A height configuration ζ has then the energy

$$H_0=-J\left[\sum_{\langle i,j\rangle} V(\zeta_i,\zeta_j)+\sum_i \zeta_i\right] , \tag{2.1}$$

where $\langle i,j\rangle$ denotes a nearest-neighbor bond, and $V(0,0)=0$, $V(0,1)=V(1,0)=0$, $V(0,2)=V(2,0)=0$, $V(1,1)=V(1,2)=V(2,1)=1$, $V(2,2)=2$. It will be convenient to have at our disposal a chemical potential μ controlling the total mass. Then

$$H=H_0-\mu\sum_i \zeta_i . \tag{2.2}$$

We note that (2.1) is a particular case of the two-dimensional Blume-Emery-Griffiths model [5]. In their notation, we have $\tilde{J}=J/2$, $\tilde{K}=J/2$, $\tilde{C}=0$, $H=3J+\mu$, $\Delta=2J$. At low temperatures, the lattice gas passes from the pure zero-phase to the pure one-phase and the pure two-phase as the chemical potential μ is increased.

Next we introduce the dynamics, which is partly mass conserving, partly mass nonconserving. Surface diffusion is governed by nearest-neighbor exchanges between heights (Kawasaki dynamics). For a given bond (i,j), the possible exchanges are $(1,0)\leftrightarrow(0,1)$, $(2,0)\leftrightarrow(1,1)$, $(0,2)\leftrightarrow(1,1)$, $(1,2)\leftrightarrow(2,1)$. Note, this implies that the only locally conserved quantity is the mass $\sum_i \zeta_i$. We denote the exchange rates by $c_{i,j}(\zeta)$ and assume that they satisfy detailed balance with respect to the energy H. This leaves us still some freedom. In our context, a physically natural choice are the Metropolis rates. Let $\Delta_{i,j}H$ be the energy difference in the exchange. Then

$$c_{i,j}(\zeta)=\begin{cases} c_0 & \text{if } \Delta_{i,j}H(\zeta)\leq 0 \\ c_0\exp[-\beta\Delta_{i,j}H(\zeta)] & \text{if } \Delta_{i,j}H(\zeta)>0 . \end{cases} \tag{2.3}$$

The exchange dynamics fixes the inverse temperature β, but leaves the chemical potential μ arbitrary. We note that an isolated atom on a terrace performs a random walk with nearest-neighbor jump rate c_0 defining an inverse "hopping time." Thus its diffusion coefficient is c_0a^2, where a denotes the lattice constant.

The external flux from the ambient atmosphere is modeled by a nonconserved Glauber-type dynamics. At each site i, the possible transitions are $0\leftrightarrow 1\leftrightarrow 2$. We denote the corresponding rates by $c_i(\zeta)$. We imagine that the incident flux is unrelated to the instantaneous height configuration. Then

$$c_i(\zeta)=c \quad \text{for } 0\rightarrow 1,\ 1\rightarrow 2 . \tag{2.4}$$

The rates for the reverse processes, $1\rightarrow 0$ and $2\rightarrow 1$, are determined by imposing detailed balance with respect to H at inverse temperature β. Physically, this means that desorption processes are governed by the local energy differences. Note that the nonconserved dynamics fixes both the temperature and chemical potential of the lattice gas.

To describe step flow, we must work with particular initial conditions and thermodynamic parameters. First, we adjust $\mu=\mu_e$ in H such that the zero-phase and the one-phase coexist. We also prepare initially a perfectly straight ledge. Then the ledge has velocity zero and thermally roughens in the course of time. To force step motion, we slightly increase c beyond its equilibrium value c_e, *without* modifying the desorption rates. Equivalently, we increase μ somewhat beyond μ_e and require the nonconserved dynamics to satisfy detailed balance with respect to that μ. Then the one-phase is favored and the ledge advances into the metastable zero-phase. Thus the TLK model can be viewed as a particular case of a *driven interface*. The interface moves with constant velocity. Our goal is to understand how the interface (ledge) roughens in the course of time.

Atoms on the back terrace have to cross a potential barrier when attaching to the ledge. This is the Schwoebel effect. In an idealized version, we may take this barrier to be infinitely high. We are then led to the one-sided version of the TLK model. It is constructed by means of obvious alterations. The height variables ζ_i take now values 0,1. The energy is the usual nearest-neighbor Ising energy

$$H=-J\sum_{\langle i,j\rangle}\zeta_i\zeta_j-(J+\mu)\sum_i\zeta_i . \tag{2.5}$$

By symmetry, phase coexistence is at $\mu_e=-3J$. The exchange dynamics is of standard form. The external flux induces the transitions $0\leftrightarrow 1$, which corresponds to spin-flips in the magnetic language. We still impose (2.4) for the transitions $0\rightarrow 1$, i.e., empty sites are filled with rate c.

If we ignore surface diffusion by setting $c_0=0$, then the one-sided model just corresponds to an Ising interface progressing into the metastable zero-phase. At low temperature, such a dynamics is equivalent either to the Eden model or to the polynuclear growth model, depending on the orientation of the ledge [6]. This is a well-understood subject [7], and it is known that the width of the ledge increases as $t^{1/3}$. Thus our goal may be re-

phrased: we try to understand how surface diffusion modifies the interface roughness.

We should count now the number of independent parameters in the TLK model. We have (i) βJ as a dimensionless inverse temperature, respectively scale of energy. (ii) The diffusion length $(x_D/a)=\sqrt{c_0/c_e}\exp[-\beta,J]$, in units of the lattice constant, of an isolated particle on a terrace. It measures how far the particle will diffuse between adsorption and desorption. Equivalently, it is the ratio of conserved to nonconserved rates. (iii) $(c-c_e)/c_e$, which tells us the quench off coexistence. Clearly, many more parameters could be introduced. An obvious physical defect is that we treat diffusion on the terrace and along the ledge on equal footing. Once at the ledge, how does a particle move around a corner? We will explore some of these possibilities on a qualitative level in Sec. VI.

We simulated the TLK model using a standard Monte Carlo algorithm. The lattice is 128×128 sites with periodic boundary conditions, and time runs up to 10^5 Monte Carlo sweeps (MCS). If the dynamics is implemented according to the rates (2.3), (2.4), and if the flux is so low as to prevent nucleation of islands on the terraces, then there is too little growth of the ledge during the available simulation time. The only way out is to suppress nucleation on the terrace by fiat. This method has been employed also in other Monte Carlo simulations of such low-temperature systems [8,9]. In Fig. 1, we show a typical configuration of the two-sided model. The atoms on the ledge are allowed to move around a corner into a kink site, i.e., an exchange between diagonally neighbored sites is allowed. Besides exclusion, there is no interaction between adatoms on the terrace.

III. THE BCF THEORY AND ITS LINEAR STABILITY

We would like to understand first under which conditions the step does not develop instabilities, i.e., remains straight on the average. This problem can be handled by a linear stability analysis of the BCF continuum theory. The role of the fluctuations will be discussed in Secs. IV and V.

Let α be a smooth curve in the plane representing the ledge. Away from the ledge, the adatom density $n=n(x,y,t)$ is governed by

$$\frac{\partial n}{\partial t}=D\Delta n-\frac{n}{\tau}+F\ . \tag{3.1}$$

Here D is the bulk diffusion coefficient, for simplicity assumed to be independent of the density, $\Delta=\nabla^2$ is the Laplacian, F is the imposed external flux, and $1/\tau$ is the desorption rate. In approximation, these constants can be related to the microscopic rates in Sec. II as $F=c/a^2$, $D=c_0a^2$, $\tau=(1/c_e)\exp[-2\beta J]$. Clearly, the density at infinity is $n_\infty=F\tau$. We have to impose boundary conditions at α. In the one-sided case, there is no flux from the back terrace, i.e.,

$$\hat{\mathbf{n}}\cdot\nabla n|_-=0\ . \tag{3.2}$$

Here $+$ $(-)$ refers to the limit from the front (back) terrace and $\hat{n}$ is the local normal to α. For the front terrace the ledge is a perfect sink. Therefore, introducing the equilibrium density n_e and imposing the Gibbs-Thomson relation,

$$(n-n_e-\Gamma\mathcal{K})|_+=0\ . \tag{3.3}$$

$\mathcal{K}$ is the local curvature of the ledge α, and $\Gamma=n_ea^2\gamma/kT$ with ledge stiffness γ and equilibrium density n_e. In the two-sided case, the ledge acts as a sink for both terraces. Therefore

$$(n-n_e-\Gamma\mathcal{K})|_\pm=0\ . \tag{3.4}$$

More generally, we could have introduced a kinetic sticking rate leading to the boundary conditions

$$D\hat{\mathbf{n}}\cdot\nabla n|_\pm=k_\pm(n-n_e-\Gamma\mathcal{K})|_\pm\ . \tag{3.5}$$

Then (3.2), (3.3) correspond to $k_+=\infty$, $k_-=0$, and (3.4) to $k_+=\infty$, $k_-=\infty$. Finally, the normal velocity of the step, v_n, is determined by the conservation of mass,

$$v_n=a^2D(\hat{\mathbf{n}}\cdot\nabla n|_+-\hat{\mathbf{n}}\cdot\nabla n|_-)\ . \tag{3.6}$$

Equations (3.1) and (3.6), together with boundary conditions (3.2), (3.3), respectively (3.4), determine the step motion.

We are looking for a solution representing a perfectly straight ledge traveling at constant velocity. This problem can be solved in full generality [2]. For our purposes, the small-velocity approximation suffices. For the two-sided case in a comoving frame of reference, it is given by

$$n_0(x,y)=\begin{cases} n_>(x,y)=n_\infty+(n_e-n_\infty)\exp[-y/x_D] & \text{if } y>0 \\ n_<(x,y)=n_\infty+(n_e-n_\infty)\exp[y/x_D] & \text{if } y<0\ . \end{cases} \tag{3.7}$$

The decay is governed by the diffusion length $x_D=\sqrt{D\tau}$. The step velocity v equals

$$v=2\frac{a^2D}{x_D}(n_\infty-n_e)\ . \tag{3.8}$$

In the one-sided case, $n_0(x,y)=n_\infty$ for $y<0$, and the velocity is one-half of that in (3.8).

We consider now a small deviation from the traveling-front solution. The ledge is then represented by a single-valued function h relative to the line $\{y=vt\}$. The density deviation f is defined by

$$f(x,y-h(x,t),t)=\begin{cases} n(x,y+vt,t)-n_>(x,y) & \text{if } y\geq h(x,t) \\ n(x,y+vt,t)-n_<(x,y) & \text{if } y<h(x,t)\ . \end{cases} \tag{3.9}$$

To first order in f and h we then obtain, in the two-sided case, the linearized equations

$$\frac{\partial f}{\partial t}=D\Delta f+v\frac{\partial f}{\partial y}-\frac{f}{\tau}\ , \tag{3.10}$$

$$f(x,0_{\pm},t)=-\Gamma\frac{\partial^2 h(x,t)}{\partial x^2}\mp\frac{n_\infty-n_e}{x_D}h(x,t)\ , \tag{3.11}$$

$$\frac{\partial h(x,t)}{\partial t}=a^2D\left[\frac{\partial f(x,0_+,t)}{\partial y}-\frac{\partial f(x,0_-,t)}{\partial y}\right]\ . \tag{3.12}$$

In the one-sided case, the latter equation has to be replaced by

$$\frac{\partial h(x,t)}{\partial t}=a^2D\left[\frac{\partial f(x,0_+,t)}{\partial y}-\frac{n_\infty-n_e}{x_D^2}h(x,t)\right]\ . \tag{3.13}$$

Equations (3.10)–(3.12) are solved by the plane-wave ansatz, $h\propto\exp[-ikx-\omega(k)t]$. In the quasistatic approximation, $\partial f/\partial t=0$, we obtain the dispersion relation

$$\omega(k)=2a^2D\Gamma\Lambda_k k^2\ , \tag{3.14}$$

with $\Lambda_k=(k^2+1/x_D^2)^{1/2}$. For the one-sided problem, the corresponding calculation yields

$$\omega(k)=-a^2D\frac{(n_\infty-n_e)}{x_D}(\Lambda_k-1/x_D)+a^2D\Gamma\Lambda_k k^2\ ; \tag{3.15}$$

compare with [10].

The quasistatic approximation is justified in all realistic cases, because the characteristic decay time of evolution for the kth mode is of order $(a^2D\Gamma\Lambda_k k^2)^{-1}$ and thus much longer than the desorption time τ. At any moment the density of adatoms can quickly adjust to the instantaneous interface configuration.

In the two-sided case the interface is always stable, whereas in the one-sided case the dispersion relation $\omega(k)$ will become negative for small k, if

$$x_D>\frac{2\Gamma}{(n_\infty-n_e)}\ . \tag{3.16}$$

The Gibbs-Thomson effect can then no longer compensate the destabilizing effect of the one-sided diffusion field. This behavior is closely related to the Mullins-Sekerka instability with the main difference due to the cutoff length scale x_D in our problem. Letting x_D approach infinity in (3.15), one obtains the Mullins-Sekerka dispersion relation with its characteristic linear behavior for small k. In Fig. 2, we show a typical configuration, where the instabilities are clearly visible. In this unstable regime individual bumps and cusps of the ledge grow deterministically.

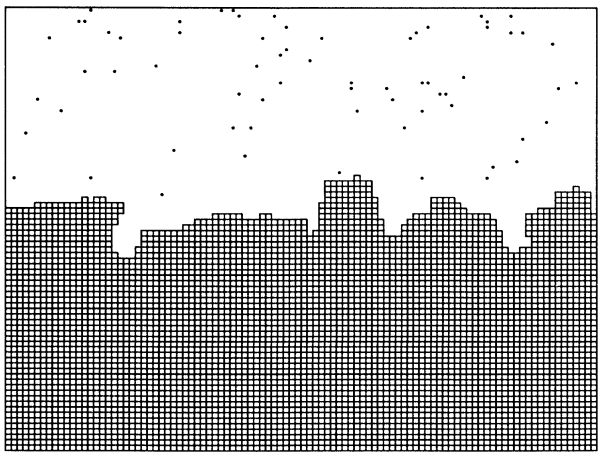

FIG. 2. Simulation of the one-sided TLK model at $t=2\times10^4$ MCS. Only adatoms on the front terrace contribute to the growth. The parameters F, x_D, βJ, and the lattice size are the same as in Fig. 1.

IV. LEDGE ROUGHENING

We consider an initially perfectly straight ledge and would like to compute how it roughens. Clearly, in the deterministic BCF theory the ledge will remain straight forever, provided the parameters are in the stable regime. Thus to have roughening, noise has to be taken into account. There are essentially three noise sources: there is shot noise from the external flux, noise associated with the diffusive motion on the terraces, and noise in adsorption and desorption processes from the ledge. The noise related to the interface is small compared to the bulk contributions. Therefore the BCF theory including noise has the form

$$\frac{\partial n(x,y,t)}{\partial t}=D\Delta n(x,y,t)-\frac{n(x,y,t)}{\tau}+F+\eta(x,y,t)\ , \tag{4.1}$$

together with boundary conditions (3.11), (3.12). η is white noise with mean zero and covariance

$$\langle\eta(\mathbf{r}_1,t_1)\eta(\mathbf{r}_2,t_2)\rangle=DF\tau\Delta\delta(\mathbf{r}_1-\mathbf{r}_2)\delta(t_1-t_2)+F\delta(\mathbf{r}_1-\mathbf{r}_2)\delta(t_1-t_2)\ . \tag{4.2}$$

The first term is due to the density fluctuations on the terraces and is therefore conservative noise, whereas the second term models the shot noise. In fact, as will be shown, on a long-time scale the shot noise will dominate.

We study first the influence of noise on the level of the linearized equations. The full nonlinear problem will be taken up in Sec. V. We linearize as in (3.10). Then

$$\frac{\partial f(x,y,t)}{\partial t}=D\Delta f(x,y,t)+v\frac{\partial f(x,y,t)}{\partial y}-\frac{f(x,y,t)}{\tau}+\eta(x,y,t)=:\mathcal{A}f+\eta\ . \tag{4.3}$$

The linearized boundary conditions (3.11)–(3.13) remain unchanged. The initial conditions are $h=0$, $f=0$. We have to compute $\langle h(x,t)^2\rangle$ for large t, where, for the sake of concreteness, we consider the two-sided case. For notational simplicity, the constants a, D, and Γ are set to unity and will be reintroduced in the final result, Eq. (4.20) below.

The boundary condition (3.11) can be satisfied by an additional source at $y=0$ in the form [11]

$$\frac{\partial}{\partial t}f(x,y,t)=\mathcal{A}f(x,y,t)+\delta(y)\frac{\partial}{\partial t}h(x,t)+\eta(x,y,t)\ . \tag{4.4}$$

Let $G(x_1,y_1,t|x_2,y_2,s)$ be the Green's function for $\partial f/\partial t=\mathcal{A}f$ without boundary conditions. Then, for $f(t=0)=0$, the solution to (4.4) reads

$$f(x_1,y_1,t)=\int_0^t ds\int\int dx_2dy_2G(x_1,y_1,t|x_2,y_2,s)\times\left[\delta(y_2)\frac{\partial}{\partial s}h(x_2,s)+\eta(x_2,y_2,s)\right]\ . \tag{4.5}$$

Adding the limits $y_1\to 0_+$, $y_1\to 0_-$, and using the second boundary condition (3.12), we obtain

$$\frac{\partial^2}{\partial x_1^2}h(x_1,t)=\int_0^t ds\int\int dx_2dy_2G(x_1,0,t|x_2,y_2,s)\times\left[\delta(y_2)\frac{\partial}{\partial s}h(x_2,s)+\eta(x_2,y_2,s)\right]\ , \tag{4.6}$$

and its Fourier transform

$$-k^2\hat{h}(k,t)=\int_0^t ds\int dq\,e^{-[k^2+q^2-ivq+(1/\tau)](t-s)}\times\left[\frac{\partial}{\partial s}\hat{h}(k,s)+\hat{\eta}(k,q,s)\right]\ , \tag{4.7}$$

where k and q are the conjugate variables to x and y, respectively. To solve for $\hat{h}$, we take the Laplace transform. Then, using that $\hat{h}(k,0)=0$, we get

$$\left[k^2+\frac{z}{[z+(v^2+k^2)]^{1/2}}\right]\hat{h}(k,z)=-\hat{\psi}(k,z)\ , \tag{4.8}$$

where we introduced the shorthand

$$v:=\left[\frac{v^2}{4}+\frac{1}{\tau}\right]^{1/2}\ . \tag{4.9}$$

Equivalently, in real time

$$\hat{h}(k,t)=-\int_0^t ds\,\alpha(t-s)\hat{\psi}(k,s)\ , \tag{4.10}$$

with

$$\hat{\psi}(k,t):=\int_0^t ds\int dq\,e^{-[k^2+q^2-ivq+(1/\tau)](t-s)}\times\hat{\eta}(k,q,s)\ .$$

$\alpha(t)$ is a memory function, which is defined implicitly by

$$\int_0^\infty dt\,e^{-zt}\alpha(t)=\left[k^2+\frac{z}{[z+(v^2+k^2)]^{1/2}}\right]^{-1}\ . \tag{4.11}$$

After these preparations, we are able to calculate the height-height correlations

$$\langle\hat{h}(k,t)[\hat{h}(k',t]^*\rangle=\int_0^t ds_1\alpha(t-s_1)\int_0^t ds_2[\alpha(t-s_2)]^*\times\langle\psi(k,s_1)[\psi(k',s_2)]^*\rangle\ . \tag{4.12}$$

If $ka\ll 1$, which is the case for a scale much greater than the lattice constant, the memory function can be approximated by

$$\alpha(t)=(v^2+k^2)^{1/2}\exp[-k^2(v^2+k^2)^{1/2}t]\ . \tag{4.13}$$

Thus

$$\langle\hat{h}(k,t)[\hat{h}(k',t)]^*\rangle=\delta(k-k')(v^2+k^2)\int_0^t ds_1e^{-k^2(v^2+k^2)^{1/2}(t-s_1)}\int_0^t ds_2e^{-k^2(v^2+k^2)^{1/2}(t-s_2)}\langle\psi(k,s_1)[\psi(k,s_2)]^*\rangle\ . \tag{4.14}$$

The integrations in (4.14) can be carried out analytically [12]. Rather than reproducing this somewhat lengthy formula, we note some reasonable approximations. First, the continuum theory is valid only for $ka\ll 1$, e.g., for wavelengths much greater than the lattice constant, and for times $t\gg\tau$, when the deterministic solution has become stationary. In addition,

$$v^2:=\frac{v^2}{4}+\frac{1}{\tau}=\frac{1}{\tau}[1+O(F\tau)^2]\ , \tag{4.15}$$

where the BCF velocity $v=(F-F_e)\sqrt{\tau}$ has been inserted. With these approximations, we obtain

$$\langle\hat{h}(k,t)[\hat{h}(k',t)]^*\rangle=\delta(k-k')\frac{\pi}{2}\frac{F\tau}{k^2}\times\{1-\exp[-2k^2(k^2+1/x_D^2)^{1/2}t]\}\ . \tag{4.16}$$

Transforming back to real space,

$$\langle h(x,t)^2\rangle=\int dk\int dk'\langle\hat{h}(k,t)[\hat{h}(k',t)]^*\rangle e^{ix(k-k')}=\int dk\langle[\hat{h}(k,t)]^2\rangle\ . \tag{4.17}$$

There are two limiting cases. If $t\ll 1/2|k|^3$, we rescale as $\kappa:=kt^{1/3}$. Then

$$\langle h(x,t)]^2\rangle=t^{1/3}\frac{\pi}{2}F\tau\int d\kappa\frac{1}{\kappa^2}(1-\exp[-2|\kappa|^3])\ . \tag{4.18}$$

For longer times $t\gg 1/2|k|^3$, we rescale as $\kappa:=kt^{1/2}$. Then

$$\langle[h(x,t)]^2\rangle=t^{1/2}\frac{\pi}{2}F\tau\int d\kappa\frac{1}{2\kappa^2}(1-\exp[-2v\kappa^2])\ . \tag{4.19}$$

We repeat the full result with the constants a, D, and Γ reinserted,

$$\langle [h(x,t)]^2 \rangle = \frac{\pi}{2} \frac{a^2 F\tau}{\Gamma} \int dk \frac{1}{k^2} \{1-\exp[-2Da^2\Gamma k^2 (k^2+1/x_D^2)^{1/2} t]\} \ . \tag{4.20}$$

The ledge roughening is governed by two power laws with exponent $\frac{1}{6}$ for small times and exponent $\frac{1}{4}$ for long times. The crossover occurs approximately at

$$t_{\rm cr} = \tau \frac{x_D}{a^2\Gamma} \ , \tag{4.21}$$

when the wavelength of typical interface fluctuations has grown up to the order of the diffusion length. The exponents $\frac{1}{6}$ and $\frac{1}{4}$ can be understood as the signatures of the conserved and nonconserved dynamics, respectively. It is known that in an Ising model with conserved dynamics (model B), the fluctuations of an initially straight interface increase to its stationary value according to a $t^{1/6}$ law [13]. Thus we have

$$\langle h(x,t)^2 \rangle \propto t^{2\beta} \ ,$$

with the scaling exponent

$$\beta = \begin{cases} \frac{1}{6} & \text{for } t \ll t_{\rm cr} \\ \frac{1}{4} & \text{for } t \gg t_{\rm cr} \ . \end{cases}$$

If we consider the stationary interface width for a sample of length L, we obtain random-walk-like fluctuations,

$$\lim_{t\to\infty} \langle h(x,t)^2 \rangle_L = \frac{\pi}{2} \frac{a^2 F\tau}{\Gamma} L \ . \tag{4.22}$$

For $F\tau = n_e$, the prefactor is the same as in a solid-on-solid (SOS) model for the thermal roughness of a single ledge [14]. In comparison to the equilibrium, this prefactor increases or decreases depending on whether there is a positive or negative growth velocity, respectively.

Our result (including the prefactor) agrees with the one obtained by Uwaha and Saito [15]. They added white noise to the deterministic dispersion relation (3.15), assuming the noise spectrum to be that of equilibrium. In contrast to their approach, we have shown that the interface fluctuations can be calculated directly from a noisy BCF theory.

In the Monte Carlo simulations, because of limited computation time, we could not verify the crossover as predicted by the linearized theory. However, we can adjust the parameters in such a way as to separately observe a $t^{1/6}$ and a $t^{1/4}$ behavior after an initial regime; see Fig. 3.

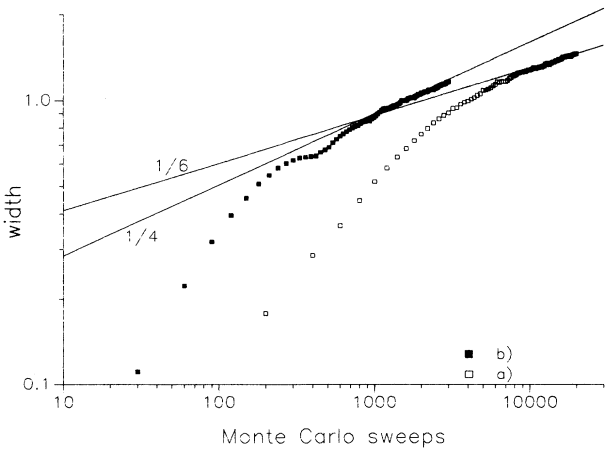

FIG. 3. Broadening of the interface width $[\langle h(t)^2 \rangle - \langle h(t) \rangle^2]^{1/2}$ for an initially straight interface. (a) Conserved dynamics only (zero external flux, no desorption) at $\beta J = 2.5$ on a 48×48 lattice. The average is over 500 runs. (b) Mixed dynamics at $F = 7\times10^{-4}$ (site$\times$MCS)$^{-1}$, $x_D = 4a$, and $\beta J = 3$ on a 64×96 lattice. The average is over 150 runs.

V. NONLINEAR THEORY

To understand the limitations of the linearized noisy BCF theory, it is useful to consider again our result (4.16) for $t > t_{\rm cr}$ when the fluctuations increase as $t^{1/4}$. Equation (4.19) is the solution of an effective Edward-Wilkinson equation [16]

$$\frac{\partial h(x)}{\partial t} = \frac{Da^2\Gamma}{x_D} \Delta h(x) + \eta(x,t) \tag{5.1}$$

with noise correlator

$$\langle \eta(x_1,t_1)\eta(x_2,t_2) \rangle = \frac{a^4 DF\tau}{x_D} \delta(x_1-x_2)\delta(t_1-t_2) \ . \tag{5.2}$$

This equation can be derived also phenomenologically simply by adding Gaussian white noise to a deterministic normal ledge velocity, which is proportional to the local curvature. Thus on a coarsened scale, $t \gg t_{\rm cr}$, $kx_D \ll 1$, the ledge motion is governed by a local equation.

From the work of KPZ [4], we know that the tilting of the ledge introduces a relevant nonlinearity that modifies the long-time scaling behavior. Thus, in a comoving frame, Eq. (5.2) has to be augmented to

$$\frac{\partial h(x,t)}{\partial t} = \frac{\lambda}{2} [\nabla h(x,t)]^2 + \sigma \Delta h(x,t) + \eta(x,t) \ . \tag{5.3}$$

Here $\sigma = Da^2\Gamma/x_D$ and the noise has strength $N = a^4 DF\tau/x_D$. For small tilt we expect the growth velocity to be isotropic. In this case [4] predicts $\lambda = v$, the BCF velocity. The nonlinearity in the KPZ equation (5.3) gives rise to a crossover from a $t^{1/4}$ to a $t^{1/3}$ broadening.

To estimate the crossover time, $t_{\rm KPZ}$, we equate the linear and nonlinear terms of (5.3) for a typical fluctuation [17]. Let us take an interface perturbation of the form $h(x) = \epsilon \sin kx$. Then

$$\frac{\lambda}{2} (\nabla h)^2 = \frac{\lambda}{2} k^2 \epsilon^2 (\cos kx)^2, \quad \sigma \Delta h = -\sigma k^2 \epsilon \sin kx \ .$$

These terms are of the same order provided $\epsilon = 2\sigma/\lambda$. Computing the initial increase of the amplitude ϵ accord-

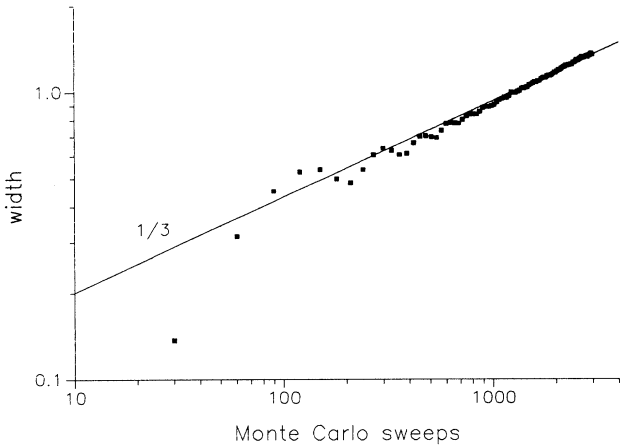

FIG. 4. Kinetic roughening in the nonlinear regime. The interface width is an average over 150 runs on a 64×96 lattice at $F=7\times10^{-4}$ (site$\times$MCS)$^{-1}$, $x_D=8a$, and $\beta J=4.5$. After an initial regime with small oscillations corresponding to the growth of a monatomic row, the roughening follows a $t^{1/3}$ power law according to the KPZ theory.

ing to (5.1), we obtain a rough estimate for the crossover time

$$t_{\mathrm{KPZ}}=\frac{1}{N^2}\frac{16\sigma^5}{\lambda^4}\ . \tag{5.4}$$

Inserting from (5.3) and $\lambda=v$, we obtain

$$t_{\mathrm{KPZ}}=\tau\frac{16\Gamma^5}{a^6\tau^6(F-F_e)^4F^2x_D}\ . \tag{5.5}$$

In Fig. 4, we have chosen the model parameters such that $t_{\mathrm{KPZ}}\simeq\tau$. Clearly, we cannot distinguish a regime described by the linearized theory, but have directly the transition to a KPZ-governed $t^{1/3}$ increase in the roughness. The small initial oscillations reflect the growth of single atomic layers.

VI. INSTABILITIES

We have seen that the one-sided TLK model becomes linearly unstable, if the high-flux condition (3.16) is satisfied. The dispersion relation $\omega(k)$ of the linear BCF theory is then negative for $0\le k\le k_c$. To access the long-time behavior, one therefore has to use the full nonlinear BCF theory. We expect that the instabilities are cut off on a length scale larger than the diffusion length x_D. On this scale, the KPZ mechanism is again in operation and one should see a roughening according to a $t^{1/3}$ law. However, in contrast to the stable case, there is no simple way to compute the coefficients λ and σ in Eq. (5.3) on a microscopic basis and to estimate thereby the crossover time t_{KPZ}.

So far we have always assumed that the hopping along the ledge is governed by the same rates as on the terraces. If we give up this restriction fractal structures can be easily produced. Such structures have been reported in scanning-tunneling-microscopy (STM) experiments [18]. Let us first consider the extreme case where ledge

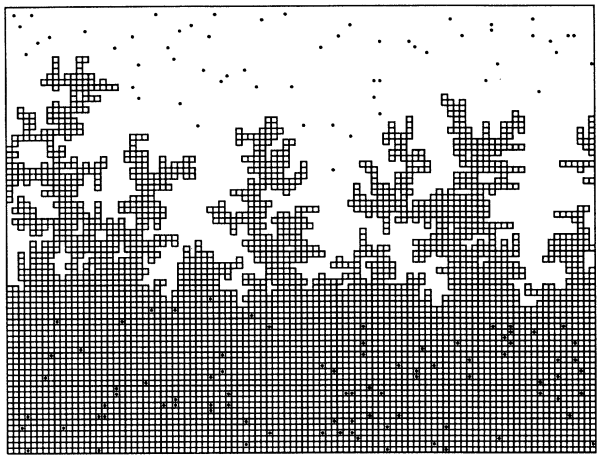

FIG. 5. Growth aggregate of a hit-and-stick process with parameters $t=8000$ MCS, $F=1.25\times10^{-4}$ (site$\times$MCS)$^{-1}$, and $x_D=20a$.

diffusion and desorption from the ledge are completely suppressed. Then atoms that hit the ledge will stick at the first site of contact. In Fig. 5, we show a typical configuration. To gain in computation time in this simulation, we actually followed the motion of individual particles. On the terrace the atoms are only subject to exclusion. We observe an aggregate with many voids and overhangs similar to the fractal geometry of diffusion-limited aggregation (DLA) [19]. However, in contrast to diffusion-limited aggregation, here we have a finite density and the additional length scale x_D cutting off the fractal geometry at larger scales.

Next let us increase somewhat the temperature. Then, just as adatoms on the terrace, atoms on the ledge perform an activated hopping process until they become finally immobilized by additional bonds to a kink site or to other diffusing atoms (nucleation on the ledge). However, we still assume the temperature to be low enough as to neglect all detachment from the ledge. The microscop-

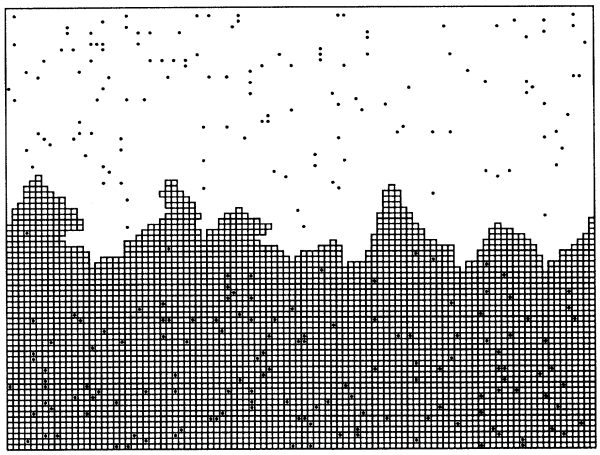

FIG. 6. One-sided ledge diffusion at the same parameters as in Fig. 5.

ic rules of ledge diffusion can change the ledge geometry in a drastic way. In analogy to the Schwoebel effect, we should distinguish the case of one- and two-sided attachment to the kink. Corresponding to the activation energies involved, moving around a corner into a kink might be kinetically blocked or not. In Fig. 6, the case of one-sided ledge diffusion is seen to give rise to intrinsic instabilities. If, on the other hand, jumps around a corner are admitted, then the ledge is essentially straight. Visually, a typical configuration cannot be distinguished from Fig. 1, which shows the case where desorption from the ledge is allowed.

VII. CONCLUSION

A crystal step moves by acquiring mass from a diffusive density field. This is an intrinsically unstable situation, since bumps and protuberances have the tendency to grow faster than pieces of the step, which lag behind. We identified two mechanisms that nevertheless suppress the fractal structure and maintain the ledge to be essentially straight. At sufficiently high temperatures, the dominant smoothening process is desorption from the ledge onto the terrace. Also, two-sided adsorption is more stabilizing than one-sided adsorption. At lower temperatures, the only mechanism in operation is ledge diffusion. We noted the importance of the "one-dimensional Schwoebel effect." If corner sites are kinetically blocked, ledge diffusion is effectively suppressed and the ledge grows unstable. If the ledge is stable, we can investigate the long-wavelength fluctuations by means of the noisy BCF theory. We obtain the standard signatures: the roughness increases as $t^{1/6}$ (conserved dynamics), $t^{1/4}$ (nonconserved dynamics), and eventually crosses over to $t^{1/3}$ (KPZ). The various regimes depend sensitively on the choice of the kinetic rates. In fact, numerically the $t^{1/3}$ growth is the most easily accessible one.

In our problem there is a cutoff by the diffusion length x_D. If one coarsens on that scale, then all the effects due to the diffusive dynamics are averaged out and absorbed into effective rates unconstrained by a conservation law. In particular, on the scale x_D, the ledge moves as in a nonconservative model. This implies that on larger scales the crystal step is governed by the KPZ equation, with effective coefficients depending on the precise microstructure.

From a theoretical point of view, it is most striking that the large variety of possible phenomena can be captured already by a two-dimensional Ising model with mixed Glauber and Kawasaki dynamics.

ACKNOWLEDGMENTS

We thank J. Krug for proposing the present problem and for useful discussions. One of us (T.S.) acknowledges the interest of R. J. Behm in this work.

[1] W. K. Burton, N. Cabrera, and F. C. Frank, Philos. Trans. R. Soc. London, Ser. A **243**, 299 (1951).
[2] R. Ghez and S. S. Iyer, IBM J. Res. Dev. **6**, 804 (1988).
[3] H. Bethge, in *Kinetics of Ordering and Growth at Surfaces,* edited by M. G. Lagally (Plenum, New York, 1990).
[4] M. Kardar, G. Parisi, and Y. C. Zhang, Phys. Rev. Lett. **56**, 889 (1986).
[5] M. Blume, V. J. Emery, and R. B. Griffiths, Phys. Rev. A **4**, 1071 (1971).
[6] P. Devillard and H. Spohn, Europhys. Lett. **17**, 113 (1992).
[7] J. Krug and H. Spohn, in *Solids Far from Equilibrium,* edited by C. Godrèche (Cambridge University Press, Cambridge, England, 1992).
[8] R. F. Xiao, J. I. D. Alexander, and F. Rosenberger, Phys. Rev. A **38**, 2447 (1988).
[9] Y. Saito and T. Ueta, Phys. Rev. A **40**, 3408 (1989).
[10] G. S. Bales and A. Zangwill, Phys. Rev. B **41**, 5500 (1990).
[11] Y. Pomeau, in *Solids Far from Equilibrium,* edited by C. Godrèche (Cambridge University Press, Cambridge, England, 1992).
[12] T. Salditt, Diplomarbeit thesis, Universität München, 1992 (unpublished).
[13] D. Jasnow and K. P. Zia, Phys. Rev. A **36**, 2243 (1987).
[14] H. J. Leamy, G. H. Filmer, and K. A. Jackson, in *Surface Physics of Materials,* edited by J. M. Blakely (Academic, New York, 1975).
[15] M. Uwaha and Y. Saito, Phys. Rev. Lett. **68**, 224 (1992).
[16] S. F. Edwards and D. R. Wilkinson, Proc. R. Soc. London, Ser. A **381**, 17 (1982).
[17] T. Bohr, G. Grinstein, C. Jayaprakash, M. H. Jensen, J. Krug, and D. Mukamel, Physica D **59**, 177 (1992).
[18] R. Q. Hwang, J. Schröder, C. Günther, and R. J. Behm, Phys. Rev. Lett. **67**, 3279 (1991).
[19] S. R. Forrest and T. A. Witten, J. Phys. A **12**, L109 (1979).